Hindawi
Advances in Meteorology
Volume 2018, Article ID 3894831, 21 pages
https://doi.org/10.1155/2018/3894831

Research Article

Comparative Analysis of Global Solar Radiation Models in Different Regions of China

Qingwen Zhang,[1] Ningbo Cui ,[1,2] Yu Feng,[1,3] Yue Jia,[4] Zhuo Li,[2] and Daozhi Gong[3]

[1]*State Key Laboratory of Hydraulics and Mountain River Engineering and College of Water Resource and Hydropower, Sichuan University, Chengdu, China*
[2]*Key Laboratory of Water Saving Agriculture in Hill Areas in Southern China of Sichuan Province, Chengdu, China*
[3]*State Engineering Laboratory of Efficient Water Use of Crops and Disaster Loss Mitigation/Key Laboratory for Dryland Agriculture, Institute of Environment and Sustainable Development in Agriculture, Chinese Academy of Agricultural Sciences, Beijing, China*
[4]*Hebei University of Water Resources and Electric Engineering, Cangzhou, China*

Correspondence should be addressed to Ningbo Cui; cuiningbo@scu.edu.cn

Received 20 November 2017; Revised 4 March 2018; Accepted 21 March 2018; Published 30 April 2018

Academic Editor: Stefania Bonafoni

Complete and accurate global solar radiation (R_s) data at a specific region are crucial for regional climate assessment and crop growth modeling. The objective of this paper was to evaluate the capability of 12 solar radiation models based on meteorological data obtained from 21 meteorological stations in China. The results showed that the estimated and measured daily R_s had statistically significant correlations ($P < 0.01$) for all the 12 models in 7 subzones of China. The Bahel model showed the best performance for daily R_s estimation among the sunshine-based models, with average R^2 of 0.910, average RMSE of 2.306 MJ m^{-2} d^{-1}, average RRMSE of 17.3%, average MAE of 1.724 MJ m^{-2} d^{-1}, and average NS of 0.895, respectively. The Bristow-Campbell (BC) model showed the best performance among the temperature-based models, with average R^2 of 0.710, average RMSE of 3.952 MJ m^{-2} d^{-1}, average RRMSE of 29.5%, average MAE of 2.958 MJ m^{-2} d^{-1}, and average NS of 0.696, respectively. On monthly scale, Ögelman model showed the best performance among the sunshine-based models, with average RE of 5.66%. The BC model showed the best performance among the temperature-based models, with average RE of 8.26%. Generally, the sunshine-based models were more accurate than the temperature-based models. Overall, the Bahel model is recommended to estimate daily R_s, Ögelman model is recommended to estimate monthly average daily R_s in China when the sunshine duration is available, and the BC model is recommended to estimate both daily R_s and monthly average daily R_s when only temperature data are available.

1. Introduction

Solar energy is the most fundamental renewable energy source on the earth's surface, and global solar radiation (R_s) plays an important role in a wide range of applications in areas such as meteorology and hydrology [1]. Changes in the amount of R_s greatly influence the hydrological cycle, terrestrial ecological systems, and the climate [2]. Complete and accurate R_s data at a specific region are highly crucial to regional crop growth modeling, evapotranspiration estimation, irrigation system development, and utilization of solar energy resources. Meanwhile, due to the fast growth in the global energy demand and destructive effects of fossil fuels on the environment, there is a growing demand for reliable R_s information for clean energy technology development [3, 4]. The best method to determine the amount of R_s at any site is to install measuring instruments such as pyranometers or pyrheliometers at every specific location. Monitoring their daily recording and maintenance, however, is a very troublesome business and costly exercise [5, 6]. In fact, the reliable measurement of R_s data is relatively scarce in many developing countries due to the expensive instruments, technical equipment, and maintenance requirements [6]. Currently, only 122 out of 752 national meteorological stations in China have R_s observing instruments [7]. Furthermore, even for those stations where R_s is observed, there are many R_s data which are missing or lie outside the expected range due to equipment failure and other difficulties [8–10].

Thus, different R_s models have been proposed for estimating daily or monthly R_s using different techniques, such as geostationary satellite images, neural networks, time series methods, physically radiative transfer models, and stochastic weather methods, which were generally based on different types of data including meteorological and geographical data [11, 12]. Among them, meteorological data-based models using empirical correlations depend on the most common meteorological elements including cloud cover, sunshine duration, temperature, and relative humidity, making them the most commonly examined and widely used models around the world, especially the sunshine-based and temperature-based models [6, 11]. The primary sunshine-based model can be traced back to Ångström model, using sunshine duration and clear sky radiation data to estimate R_s [11, 13, 14]. Prescott [15] suggested using the extraterrestrial radiation to replace clear sky radiation and presented the Ångström-Prescott (AP) model. Several Ångström-type regression models, namely, the linear, quadratic, cubic, logarithmic, and exponential models, were compared to estimate R_s on horizontal surfaces at 4 meteorological stations in Tunisia, and the statistical results indicated that the models were considered suited to accurately estimate R_s, and the cubic model showed the best regression fit and performed slightly better than the others [16]. Although the sunshine-based models are generally more accurate for estimating R_s, their application is often limited by the lack of sunshine records [1, 9, 17]. In this context, R_s forecast models based on geographical location, air temperature, and/or precipitation, recorded at the great majority of the meteorological stations, are attractive and viable options [1, 8]. The temperature-based models were only based on air temperature data which can be measured easily [18]. Hargreaves-Samani (HS) model [19] was proposed as a more convenient, effective, and strong applicability model with fewer input parameters, based on the daily maximum and minimum temperature to estimate R_s. Annandale et al. [20] modified the HS model by accounting for the effects of reduced altitude and atmosphere thickness on R_s. In order to calculate the average monthly R_s, Allen [21, 22] also proposed a self-calibrated model based on HS model. Bristow and Campbell [23] presented a simple model for estimating daily R_s, in which R_s was an exponential function in terms of temperature. Goodin et al. [24] modified Bristow-Campbell (BC) model by adding the extraterrestrial R_s term meant to act as a scaling factor. Liu et al. [10] evaluated the accuracy and applicability of 16 temperature-based models, including modified versions of the BC and HS models in 15 meteorological stations of Northeast China, North China Plain, and Northwest China, and the results showed that the original BC model performed similarly to the best performing modified HS model but significantly outperformed the original HS model with a 4~7% higher accuracy. Hassan et al. [11] established 17 new temperature-based models and compared these models with Annandale, Allen, and Goodin models to estimate monthly average daily R_s in Egypt and found that the local formula for the most accurate new model provided good predictions at different locations, especially at coastal sites. In general, the sunshine-based models are more accurate than temperature-based models [11, 25]. However, sunshine data are not widely available compared with ambient temperature data at standard meteorological stations [11].

China is an agricultural country, and agricultural application of solar energy has an important guiding significance to the agricultural clean production, energy conservation, and emissions reduction. Therefore, reliable estimation of R_s is very important for the operation of solar-powered pump station systems and solar irrigation systems, lift irrigated projects, and potential yield of crops in China [17]. In particular, it is of great significance for developing and utilizing solar energy resources in nonradiation observation areas due to the lack of observation stations and meteorological stations. In this paper, we analyzed the accuracy and applicability of 9 sunshine-based models and 3 temperature-based models to estimate daily R_s using the widely measured meteorological variable obtained from 21 meteorological stations in China, and the empirical coefficients of each model were calibrated based on the least squares method.

2. Materials and Methods

2.1. Study Area and Experimental Data. According to the natural geographical features, China is divided into 7 subzones: North China, Central China, East China, South China, Northeast, Northwest, and Southwest China. In the current study, 21 meteorological stations located in different climatic zones of China were selected (Figure 1), and each subzone contains 3 meteorological stations.

Daily measurements of global solar radiation (R_s) and meteorological variables, including maximum ($T_{\max}$) and minimum ($T_{\min}$) air temperature at 2 m height, relative humidity (RH), and sunshine duration (n) were obtained from 21 national meteorological stations during 1995~2014. The data of 1995~2010 were used to calibrate the empirical coefficients of the 12 models and the data of 2011~2014 were used to evaluate the performance of the models. The data sets were provided and rigorously quality-controlled by the National Meteorological Information Center of China Meteorological Administration (http://data.cma.cn/). Missing data were reconstructed based on linear interpolation. The geographical locations of each station and annual mean meteorological variables are presented in Table 1.

2.2. Models for Estimation of Solar Radiation. A number of empirical correlations which determine the relation between R_s and various meteorological parameters have been developed to estimate daily or monthly R_s in the literature, such as sunshine-based models, cloud-based models, temperature-based models, and other meteorological parameter-based models [6, 26]. The sunshine-based and temperature-based models are the most commonly used around the world [6, 9]. In this paper, 12 representative models were chosen to predict R_s, including 9 sunshine-based models and 3 temperature-based models.

2.2.1. Sunshine-Based Models

Model 1 (Ångström-Prescott model (AP)). Ångström [14] derived a simple linear relationship between the ratio of

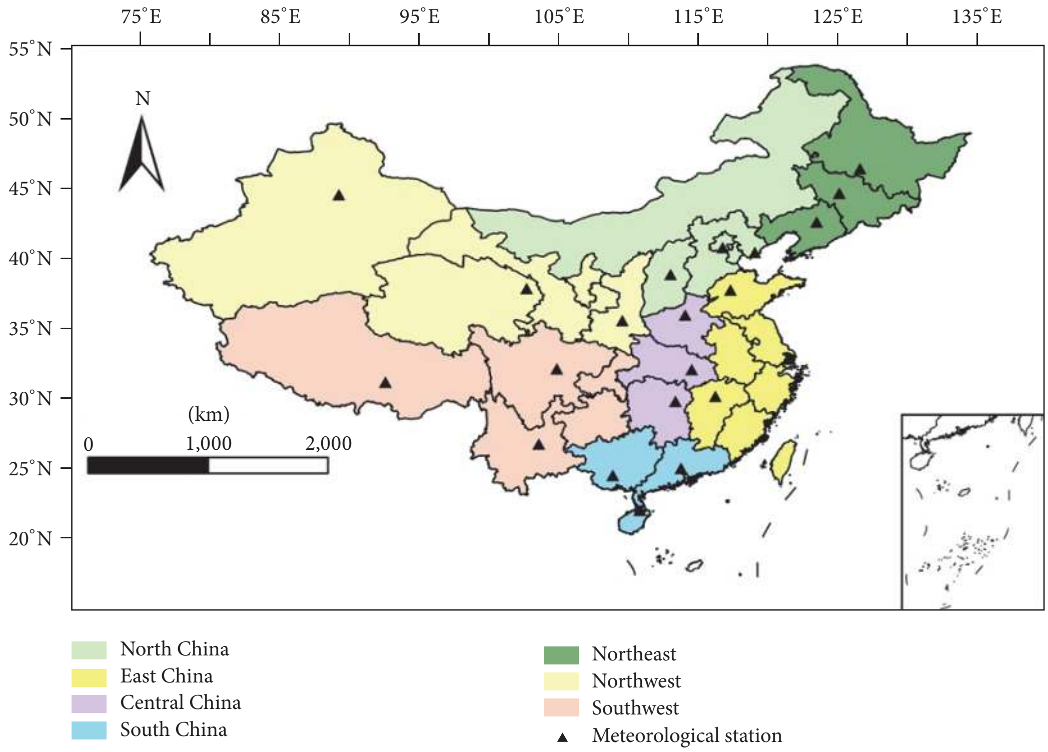

Figure 1: Geographical positions of the meteorological stations.

average daily R_s and the corresponding value on a completely clear day at a given location and the ratio of average daily sunshine duration to the maximum possible sunshine duration, which is the most widely used correlation for estimating daily R_s [27]. Prescott [15] modified the method and proposed the following equation:

$$R_s = \left[a + b\left(\frac{n}{N}\right)\right] \times R_a, \quad (1)$$

where R_s is the global solar radiation (MJ m^{-2} d^{-1}), R_a is the extraterrestrial radiation (MJ m^{-2} d^{-1}), n is sunshine duration (h), N is maximum possible sunshine duration (h), and a and b are the empirical coefficients.

Model 2 (Ögelman model (OG)). Ögelman et al. [28] suggested a second-order polynomial equation for estimating R_s as follows:

$$R_s = \left[a + b\left(\frac{n}{N}\right) + c\left(\frac{n}{N}\right)^2\right] \times R_a, \quad (2)$$

where a, b, and c are the empirical coefficients.

Model 3 (Jin model (Jin)). Through the use of R_s data and some geographical parameters like altitude and latitude, Jin et al. [29] derived the following model:

$$R_s = \left[a + b\cos\varphi + cZ + d\left(\frac{n}{N}\right)\right] \times R_a, \quad (3)$$

where φ is the latitude of the location (°) and Z is the altitude of the location (km); a, b, c, and d are the empirical coefficients.

Model 4 (Bahel model (BA)). Bahel et al. [30] suggested a famous correlation with varied meteorological conditions and a wide distribution of geographic location; the equation is as follows:

$$R_s = \left[a + b\left(\frac{n}{N}\right) + c\left(\frac{n}{N}\right)^2 + d\left(\frac{n}{N}\right)^3\right] \times R_a, \quad (4)$$

where a, b, c, and d are the empirical coefficients.

Model 5 (Louche model (LO)). Louche et al. [31] have modified the Ångström-Prescott model through the use of the ratio of (n/N_{nh}) instead of (n/N); the equation is presented as follows:

$$R_s = \left[a + b\left(\frac{n}{N_{nh}}\right)\right] \times R_a,$$
$$\frac{1}{N_{nh}} = \frac{0.8706}{N} + 0.0003, \quad (5)$$

where a and b are the empirical coefficients.

Model 6 (Glover-McCulloch model (GM)). Glover and McCulloch [32] suggested the following model, which took into account the effect of latitude of the site φ as an additional input and was valid for $\varphi < 60°$:

$$R_s = \left[a\cos\varphi + b\left(\frac{n}{N}\right)\right] \times R_a, \quad (6)$$

where a and b are the empirical coefficients.

Table 1: The geographical locations of each radiation station and its annual mean meteorological parameters.

Subzones	WMO number	Station	Latitude (°N)	Longitude (°E)	Altitude (m)	T_{max} (°C)	T_{min} (°C)	n (h)	RH (%)	R_s (MJ m^{-2} d^{-1})
	54511	Beijing	39.8	116.5	31.3	18.5	8.4	6.7	53.4	13.5
North China	54539	Laoting	39.4	118.9	10.5	17.0	7.4	6.6	64.1	13.9
	53772	Taiyuan	37.8	112.6	778.3	17.8	5.3	6.7	55.8	13.6
	57494	Wuhan	30.6	114.1	23.1	22.0	14.2	5.0	74.2	11.7
Central China	57687	Changsha	28.2	112.9	68.0	22.2	15.0	4.3	76.0	10.8
	57083	Zhengzhou	34.7	113.7	110.4	21.2	10.8	5.1	61.2	12.8
	54823	Jinan	36.6	117.1	170.3	19.8	10.8	6.0	56.7	13.2
East China	58606	Nanchang	28.6	115.9	46.9	22.4	15.5	5.0	74.0	12.1
	58362	Shanghai	31.4	121.5	5.5	20.8	14.3	4.8	72.6	12.5
	59287	Guangzhou	23.2	113.3	41.0	26.9	19.3	4.3	74.8	11.7
South China	59758	Haikou	20.0	110.3	63.5	28.4	22.1	5.0	81.5	14.1
	59431	Nanning	22.6	108.2	121.6	26.5	18.5	4.1	78.8	12.4
	50953	Harbin	45.8	126.8	142.3	10.7	0.2	6.3	63.6	12.9
Northeast China	54342	Shenyang	41.7	123.5	49.0	14.4	3.2	6.5	63.9	13.4
	54161	Changchun	43.9	125.2	236.8	11.7	1.7	7.0	60.8	13.4
	51463	Urumqi	43.8	87.7	935.0	13.2	3.7	7.3	56.2	14.1
Northwest China	57036	Hsian	34.3	108.9	397.5	20.1	10.6	4.7	64.0	12.0
	52866	Xining	36.7	101.8	2295.2	14.5	−0.4	6.9	58.2	15.6
	56294	Chengdu	30.7	104.0	506.1	20.9	13.6	2.6	77.7	9.3
Southwest China	56778	Kunming	25.0	102.7	1886.5	21.8	11.8	6.0	68.3	15.4
	55591	Lasa	29.7	91.1	3648.9	16.8	3.1	8.2	40.3	20.4

Model 7 (Elagib-Mansell model (EM)). Through the use of sunshine duration and geographical parameters, Elagib and Mansell [33] derived a new equation for estimating R_s as

$$R_s = \left[a + bL + cZ + d\left(\frac{n}{N}\right)\right] \times R_a, \tag{7}$$

where L is the latitude of the location (rad); a, b, c, and d are the empirical coefficients.

Model 8 (Almorox-Hontoria model (AH)). Almorox and Hontoria [34] derived an exponential type equation as follows:

$$R_s = \left[a + b\exp\left(\frac{n}{N}\right)\right] \times R_a, \tag{8}$$

where a and b are the empirical coefficients.

Model 9 (Dogniaux-Lemoine model (DL)). Through taking into account the effect of latitude of the site as an additional input, Dogniaux and Lemoine [35] derived the following equation for estimating R_s:

$$R_s = \left\{a + \left[b\left(\frac{n}{N}\right) + c\right]L + d\left(\frac{n}{N}\right)\right\} \times R_a, \tag{9}$$

where a, b, c, and d are the empirical coefficients.

2.2.2. Temperature-Based Models

Model 10 (Hargreaves-Samani model (HS)). Hargreaves and Samani [19, 36] recommended a simple equation to estimate R_s which required only maximum and minimum temperature data; the equation is presented as follows:

$$R_s = \left[a\left(T_{\max} - T_{\min}\right)^{0.5}\right] \times R_a, \tag{10}$$

where $T_{\max}$ and $T_{\min}$ are the maximum daily temperature and minimum daily temperature (°), respectively; a is the empirical coefficient.

Model 11 (Annandale model (AN)). Annandale et al. [20] derived a model based on Hargreaves-Samani model by accounting for the effects of reduced altitude and atmospheric thickness on R_s; the equation is presented as follows:

$$R_s = \left[a\left(1 + 2.7 \times 10^{-5}Z\right)\left(T_{\max} - T_{\min}\right)^{0.5}\right] \times R_a, \tag{11}$$

where a is the empirical coefficient.

Model 12 (Bristow-Campbell model (BC)). Bristow and Campbell [23] proposed a method for daily R_s based on the difference of maximum and minimum temperatures; the equation is presented as follows:

$$R_s = a\left[1 - \exp\left(-b\left(T_{\max} - T_{\min}\right)^{c}\right)\right] \times R_a, \tag{12}$$

where a, b, and c are the empirical coefficients.

2.3. Statistical Evaluation. The performance of the studied models to estimate R_s was evaluated in terms of the following statistical error tests: coefficient of determination (R^2), root mean square error (RMSE), relative root mean square error (RRMSE), Nash–Sutcliffe coefficient (NS), and mean absolute error (MAE), which are defined in the following equations [37, 38]:

$$\begin{aligned}
R^2 &= \frac{\left[\sum_{i=1}^{n}\left(X_i - \overline{X}\right)\left(Y_i - \overline{Y}\right)\right]^2}{\sum_{i=1}^{n}\left(X_i - \overline{X}\right)^2 \sum_{i=1}^{n}\left(Y_i - \overline{Y}\right)^2}, \\
\text{RMSE} &= \sqrt{\frac{1}{n}\sum_{i=1}^{n}\left(Y_i - X_i\right)^2}, \\
\text{RRMSE} &= \frac{\sqrt{(1/n)\sum_{i=1}^{n}\left(Y_i - X_i\right)^2}}{\overline{X}}, \\
\text{NS} &= 1 - \frac{\sum_{i=1}^{n}\left(Y_i - X_i\right)^2}{\sum_{i=1}^{n}\left(X_i - \overline{X}\right)^2}, \\
\text{MAE} &= \frac{1}{n}\sum_{i=1}^{n}\left|Y_i - X_i\right|,
\end{aligned} \tag{13}$$

where X_i and Y_i denote the measured and estimated values, $\overline{X_i}$ and $\overline{Y_i}$ represent the corresponding mean R_s values, respectively, the subscript i refers to the ith value of the solar irradiation, and n is the number of data. RMSE and MAE are both in $\mathrm{MJ\,m^{-2}\,d^{-1}}$; RRMSE is dimensionless, taking on a value from 0 (perfect fit) to ∞ (the worst fit); NS is dimensionless, taking on a value from 1 (perfect fit) to $-\infty$ (the worst fit).

2.4. Global Performance Indicator. In order to overcome the discrepancy and to further improve the outcomes of statistical analysis, a new factor was proposed by Despotovic et al. [39] known as the Global Performance Indicator (GPI), which was a worthy tool to combine the effects of individual statistical indicators. The equation is presented as follows:

$$\text{GPI}_i = \sum_{j=1}^{5}\alpha_j\left(y_j - y_{ij}\right), \tag{14}$$

where α_j is equal to −1 for the indicator R^2 and NS, while for other indicators it is equal to +1. y_j is the median of scaled values of indicator j, and y_{ij} is the scaled value of indicator j for model i. A higher value of GPI results in a higher accuracy of the model.

3. Results

3.1. Calibration of Empirical Coefficients. The empirical coefficients of the 12 models were calibrated based on the least squares method for R_s estimation using the meteorological variables obtained from 21 meteorological stations during 1995~2010, and the adjusted coefficients of each subzone are shown in Table 2. As shown in Table 2, the calibrated a and b of the AP model ranged between 0.161~0.214 and 0.532~0.555, respectively. The calibrated a, b, and c of the OG model ranged between 0.144~0.202, 0.605~0.798, and −0.313~−0.082, respectively. The calibrated a, b, c, and d of Jin model ranged between 1.805~2.068, −2.227~−2.048, −0.101~0.027, and 0.532~0.555, respectively. The calibrated a, b, c, and d of the BA model ranged between 0.134~0.190, 0.867~1.261, −1.799~−0.739, and 0.443~1.158, respectively. The calibrated a and b of the LO model ranged between 0.161~0.214 and 0.608~0.635, respectively. The calibrated a and b of the GM model ranged between 0.185~0.269 and 0.532~0.555, respectively. The calibrated a, b, c, and d of the EM model ranged between 0.130~0.163, 0.005~0.034, 0.029~0.037, and 0.532~0.555, respectively. The calibrated a and b of the AH model ranged between −0.165~−0.085 and 0.325~0.358, respectively. The calibrated a, b, c, and d of the DL model ranged between 0.198~0.260, 0.082~0.109, −0.090~−0.065, and 0.456~0.524, respectively. The calibrated a of HS and AN models were both in the range 0.139~0.155. The calibrated a, b, and c of the BC model ranged between 0.552~0.695, 0.018~0.030, and 1.740~2.269, respectively. The regression coefficients were different in different climate zones. This can be explained as a consequence of local and seasonal changes in the type and thickness of cloud cover, the effects of snow covered surfaces, the concentrations of pollutants, and latitude [6, 34, 40].

3.2. Performances of the Models. The statistic performances of the analyzed models in estimating daily R_s for each zone of China are shown in Tables 3–9. As shown in Tables 3–9, there were good agreements between the estimations and the measurements. The estimated and measured daily R_s had statistically significant correlations for all the 12 models at the 21 meteorological stations ($P < 0.01$). The statistical results showed that the sunshine-based models were more accurate for daily R_s estimation at the 7 subzones of China compared with the temperature-based models.

In North China, the BA model had the best estimation precision among the sunshine-based models, followed by Jin and DL models, with average R^2 of 0.923, 0.921, and 0.921, average RMSE of 2.209, 2.231, and 2.231 MJ m^{-2} d^{-1}, average RRMSE of 15.5%, 15.6%, and 15.6%, average MAE of 1.603, 1.639, and 1.639 MJ m^{-2} d^{-1}, average NS of 0.906, 0.904, and 0.904, and GPI of 0.069, 0.011, and 0.011, respectively. The BC model showed the highest estimation precision among the temperature-based models, with average R^2 of 0.735, average RMSE of 3.953 MJ m^{-2} d^{-1}, average RRMSE of 27.8%, average MAE of 3.007 MJ m^{-2} d^{-1}, average NS of 0.703, and GPI of −4.084.

In Central China, the BA model had the best estimation precision compared with other sunshine-based models, followed by OG and LO models, with average R^2 of 0.906, 0.898, and 0.896, average RMSE of 2.368, 2.445, and 2.482 MJ m^{-2} d^{-1}, average RRMSE of 19.8%, 20.5%, and 20.8%, average MAE of 1.751, 1.833, and 1.873 MJ m^{-2} d^{-1}, average NS of 0.899, 0.892, and 0.889, and GPI of 0.236, 0.078, and 0.002, respectively. The BC model showed the best estimation precision among the temperature-based models, with average R^2 of 0.701, average RMSE of 4.170 MJ m^{-2} d^{-1}, average RRMSE of 35.0%, average MAE of 3.021 MJ m^{-2} d^{-1}, average NS of 0.693, and GPI of −3.485.

In Eastern China, the BA model showed the best estimation precision compared with other sunshine-based models, followed by OG and DL models, with average R^2 of 0.914, 0.909, and 0.900, average RMSE of 2.325, 2.397, and 2.458 MJ m^{-2} d^{-1}, average RRMSE of 17.7%, 18.3%, and 18.8%, average MAE of 1.730, 1.812, and 1.851 MJ m^{-2} d^{-1}, average NS of 0.901, 0.895, and 0.890, and GPI of 0.284, 0.160, and 0.035, respectively. The BC model showed the best performance among the temperature-based models, with average R^2 of 0.640, average RMSE of 4.582 MJ m^{-2} d^{-1}, average RRMSE of 34.9%, average MAE of 3.449 MJ m^{-2} d^{-1}, average NS of 0.616, and GPI of −3.838.

In South China, the BA model showed the highest prediction accuracy among the sunshine-based models, followed by OG and LO models, with average R^2 of 0.911, 0.904, and 0.897, average RMSE of 2.222, 2.299, and 2.343 MJ m^{-2} d^{-1}, average RRMSE of 16.7%, 17.3%, and 17.7%, average MAE of 1.776, 1.850, and 1.885 MJ m^{-2} d^{-1}, average NS of 0.898, 0.891, and 0.888, and GPI of 0.278, 0.127, and 0.035, respectively. The BC model had the best estimation precision compared with the other temperature-based models, with average R^2 of 0.696, average RMSE of 3.937 MJ m^{-2} d^{-1}, average RRMSE of 29.6%, average MAE of 3.064 MJ m^{-2} d^{-1}, average NS of 0.685, and GPI of −3.273.

In Northeast China, the BA model had the best estimation precision compared with other sunshine-based models, followed by OG and AP models, with average R^2 of 0.921, 0.920, and 0.918, average RMSE of 2.224, 2.230, and 2.252 MJ m^{-2} d^{-1}, average RRMSE of 16.3%, 16.3%, and 16.5%, average MAE of 1.661, 1.669, and 1.685 MJ m^{-2} d^{-1}, average NS of 0.904, 0.904, and 0.902, and GPI of 0.072, 0.055, and 0.003, respectively. The BC model had the highest estimation precision among the temperature-based models, with average R^2 of 0.718, average RMSE of 3.944 MJ m^{-2} d^{-1}, average RRMSE of 28.8%, average MAE of 2.955 MJ m^{-2} d^{-1}, average NS of 0.708, and GPI of −4.275.

In Northwest China, the BA model showed the highest prediction accuracy among the sunshine-based models, followed by OG and EM models, with average R^2 of 0.890, 0.888, and 0.888, average RMSE of 2.665, 2.684, and 2.693 MJ m^{-2} d^{-1}, average RRMSE of 19.4%, 19.5%, and 19.6%, average MAE of 1.932, 1.956, and 1.941 MJ m^{-2} d^{-1}, average NS of 0.881, 0.879, and 0.878, and GPI of 0.071, 0.013, and 0.010, respectively. The BC model had the best estimation precision compared with the temperature-based models, with average R^2 of 0.729, average RMSE of 4.075 MJ m^{-2} d^{-1}, average RRMSE of 29.4%, average MAE of 2.940 MJ m^{-2} d^{-1}, average NS of 0.724, and GPI of −3.787.

In Southwest China, the BA model had the best estimation precision compared with other sunshine-based models, followed by OG and AP models, with average R^2 of 0.904, 0.898, and 0.895, average RMSE of 2.132, 2.163, and 2.206 MJ m^{-2} d^{-1}, average RRMSE of 15.7%, 16.0%, and

Table 2: Calibration empirical coefficients for the studied models in different subzones of China.

Model	Coefficient	North China	Central China	East China	South China	Northeast	Northwest	Southwest
Ångström-Prescott (AP)	a	0.182	0.161	0.167	0.171	0.193	0.193	0.214
	b	0.532	0.543	0.551	0.555	0.540	0.545	0.552
Ögelman (OG)	a	0.174	0.144	0.149	0.154	0.180	0.180	0.202
	b	0.605	0.798	0.785	0.793	0.655	0.685	0.685
	c	−0.082	−0.313	−0.283	−0.307	−0.126	−0.163	−0.167
Jin	a	1.896	1.975	1.965	2.068	1.805	1.977	2.061
	b	−2.174	−2.124	−2.130	−2.048	−2.227	−2.110	−2.052
	c	−0.018	0.021	0.016	0.027	−0.015	−0.101	−0.027
	d	0.532	0.543	0.551	0.555	0.540	0.545	0.552
Bahel (BA)	a	0.160	0.134	0.138	0.142	0.171	0.174	0.190
	b	1.011	1.261	1.209	1.224	0.867	0.912	0.992
	c	−1.265	−1.799	−1.610	−1.745	−0.739	−0.860	−1.148
	d	0.856	1.147	1.006	1.158	0.443	0.524	0.776
Louche (LO)	a	0.182	0.161	0.167	0.171	0.193	0.193	0.214
	b	0.608	0.621	0.630	0.635	0.617	0.623	0.631
Glover-McCulloch (GM)	a	0.234	0.189	0.198	0.185	0.269	0.246	0.244
	b	0.532	0.543	0.551	0.555	0.540	0.545	0.552
Elagib-Mansell (EM)	a	0.154	0.149	0.154	0.163	0.163	0.142	0.130
	b	0.024	0.017	0.016	0.018	0.034	0.013	0.005
	c	0.032	0.030	0.030	0.029	0.030	0.037	0.037
	d	0.532	0.543	0.551	0.555	0.540	0.545	0.552
Almorox-Hontoria (AH)	a	−0.114	−0.165	−0.156	−0.165	−0.099	−0.107	−0.085
	b	0.325	0.344	0.345	0.358	0.325	0.331	0.336
Dogniaux-Lemoine (DL)	a	0.243	0.209	0.216	0.198	0.260	0.252	0.246
	b	0.102	0.097	0.101	0.082	0.109	0.108	0.095
	c	−0.090	−0.089	−0.088	−0.069	−0.087	−0.088	−0.065
	d	0.462	0.490	0.494	0.524	0.456	0.471	0.504
Hargreaves-Samani (HS)	a	0.148	0.139	0.155	0.148	0.153	0.148	0.149
Annandale (AN)	a	0.148	0.139	0.155	0.148	0.153	0.148	0.149
Bristow-Campbell (BC)	a	0.602	0.552	0.552	0.561	0.619	0.647	0.695
	b	0.023	0.018	0.025	0.028	0.030	0.027	0.019
	c	1.872	2.194	2.269	2.051	1.801	1.740	1.848

Table 3: Statistics performances of the 12 models in estimating global solar radiation in North China.

Stations	Evaluation index	AP	OG	Jin	BA	LO	GM	EM	AH	DL	HS	AN	BC
Beijing	R^2	0.928**	0.928**	0.928**	0.930**	0.928**	0.928**	0.928**	0.921**	0.928**	0.659**	0.659**	0.710**
	RMSE	2.030	2.037	2.028	2.007	2.027	2.029	2.035	2.103	2.027	4.273	4.273	3.965
	RRMSE	14.7	14.7	14.7	14.5	14.7	14.7	14.7	15.2	14.7	30.9	30.9	28.7
	NS	0.921	0.921	0.921	0.923	0.921	0.921	0.921	0.915	0.921	0.651	0.651	0.699
	MAE	1.463	1.471	1.461	1.404	1.459	1.462	1.467	1.505	1.459	3.314	3.314	2.986
Laoting	R^2	0.929**	0.928**	0.929**	0.929**	0.929**	0.929**	0.929**	0.920**	0.929**	0.690**	0.690**	0.747**
	RMSE	1.866	1.878	1.863	1.855	1.866	1.867	1.868	1.971	1.863	3.866	3.866	3.493
	RRMSE	13.5	13.6	13.5	13.5	13.5	13.6	13.6	14.3	13.5	28.1	28.1	25.4
	NS	0.927	0.927	0.928	0.928	0.927	0.927	0.927	0.919	0.928	0.689	0.689	0.746
	MAE	1.350	1.374	1.348	1.335	1.349	1.351	1.351	1.401	1.348	2.991	2.991	2.665
Taiyuan	R^2	0.906**	0.905**	0.906**	0.909**	0.906**	0.906**	0.906**	0.901**	0.906**	0.709**	0.709**	0.747**
	RMSE	2.809	2.814	2.802	2.765	2.802	2.806	2.814	2.828	2.804	4.592	4.592	4.400
	RRMSE	18.7	18.7	18.7	18.4	18.7	18.7	18.7	18.8	18.7	30.6	30.6	29.3
	NS	0.864	0.863	0.864	0.868	0.864	0.864	0.863	0.862	0.864	0.635	0.635	0.665
	MAE	2.115	2.121	2.109	2.070	2.110	2.113	2.119	2.118	2.111	3.579	3.579	3.370
Average	R^2	0.921**	0.920**	0.921**	0.923**	0.921**	0.921**	0.921**	0.914**	0.921**	0.686**	0.686**	0.735**
	RMSE	2.235	2.243	2.231	2.209	2.232	2.234	2.239	2.301	2.231	4.244	4.244	3.953
	RRMSE	15.6	15.7	15.6	15.5	15.6	15.6	15.7	16.1	15.6	29.9	29.9	27.8
	NS	0.904	0.903	0.904	0.906	0.904	0.904	0.904	0.899	0.904	0.658	0.658	0.703
	MAE	1.643	1.655	1.639	1.603	1.640	1.642	1.646	1.675	1.639	3.295	3.295	3.007
	GPI	0.003	−0.017	0.011	0.069	0.010	0.006	−0.003	−0.130	0.011	−4.931	−4.931	−4.084
	Rank	6	8	2	1	4	5	7	9	3	12	11	10

Note. R^2, NS, and GPI are dimensionless; RRMSE is a percentage (%); RMSE and MAE are both in MJ m^{-1} d^{-1}; ∗∗ means a statistically significant correlation ($P < 0.01$) (the same as shown in Tables 4–9).

Table 4: Statistics performances of the 12 models in estimating global solar radiation in Central China.

Stations	Evaluation index	AP	OG	Jin	BA	LO	GM	EM	AH	DL	HS	AN	BC
	R^2	0.850**	0.857**	0.850**	0.863**	0.850**	0.850**	0.850**	0.830**	0.850**	0.644**	0.644**	0.647**
	RMSE	3.141	3.067	3.147	3.016	3.142	3.147	3.142	3.340	3.142	5.141	5.141	4.709
Wuhan	RRMSE	26.1	25.4	26.1	25.0	26.1	26.1	26.1	27.7	26.1	42.6	42.6	39.1
	NS	0.839	0.846	0.838	0.851	0.839	0.838	0.838	0.818	0.838	0.568	0.568	0.637
	MAE	2.326	2.219	2.333	2.166	2.329	2.333	2.328	2.544	2.329	3.998	3.998	3.380
	R^2	0.935**	0.931**	0.935**	0.937**	0.935**	0.935**	0.935**	0.921**	0.935**	0.675**	0.675**	0.731**
	RMSE	2.062	2.085	2.066	2.018	2.060	2.061	2.062	2.292	2.063	4.874	4.874	4.047
Changsha	RRMSE	18.9	19.1	19.0	18.5	18.9	18.9	18.9	21.0	18.9	44.7	44.7	37.1
	NS	0.927	0.926	0.927	0.930	0.928	0.927	0.927	0.910	0.927	0.594	0.594	0.720
	MAE	1.648	1.676	1.651	1.602	1.646	1.648	1.648	1.846	1.649	3.984	3.984	2.903
	R^2	0.902**	0.908**	0.902**	0.917**	0.902**	0.902**	0.902**	0.883**	0.902**	0.688**	0.688**	0.727**
	RMSE	2.246	2.182	2.244	2.069	2.246	2.244	2.245	2.436	2.243	4.180	4.180	3.753
Zhengzhou	RRMSE	17.3	16.8	17.3	15.9	17.3	17.3	17.3	18.8	17.3	32.2	32.2	28.9
	NS	0.900	0.906	0.900	0.915	0.900	0.900	0.900	0.882	0.900	0.653	0.653	0.721
	MAE	1.646	1.606	1.644	1.484	1.645	1.644	1.645	1.818	1.643	3.269	3.269	2.780
	R^2	0.896**	0.898**	0.896**	0.906**	0.896**	0.896**	0.896**	0.878**	0.896**	0.669**	0.669**	0.701**
	RMSE	2.483	2.445	2.486	2.368	2.482	2.484	2.483	2.689	2.483	4.732	4.732	4.170
	RRMSE	20.8	20.5	20.8	19.8	20.8	20.8	20.8	22.5	20.8	39.9	39.9	35.0
Average	NS	0.889	0.892	0.888	0.899	0.889	0.889	0.889	0.870	0.889	0.605	0.605	0.693
	MAE	1.873	1.833	1.876	1.751	1.873	1.875	1.874	2.069	1.874	3.751	3.751	3.021
	GPI	0.001	0.078	−0.003	0.236	0.002	−0.001	0.001	−0.407	0.002	−4.764	−4.764	−3.485
	Rank	5	2	8	1	3	7	6	9	4	12	11	10

Table 5: Statistics performances of the 12 models in estimating global solar radiation in Eastern China.

Stations	Evaluation index	AP	OG	Jin	BA	LO	GM	EM	AH	DL	HS	AN	BC
Jinan	R^2	0.906**	0.908**	0.906**	0.912**	0.906**	0.906**	0.906**	0.891**	0.907**	0.610**	0.610**	0.665**
	RMSE	2.565	2.565	2.558	2.491	2.570	2.523	2.569	2.679	2.456	4.828	4.828	4.592
	RRMSE	18.0	18.0	18.0	17.5	18.0	17.7	18.0	18.8	17.2	33.9	33.9	32.2
	NS	0.876	0.876	0.877	0.883	0.875	0.880	0.876	0.865	0.886	0.561	0.561	0.603
	MAE	1.971	1.978	1.965	1.894	1.977	1.931	1.975	2.049	1.867	3.904	3.904	3.578
Nanchang	R^2	0.898**	0.903**	0.898**	0.908**	0.898**	0.898**	0.898**	0.879**	0.898**	0.619**	0.619**	0.682**
	RMSE	2.507	2.449	2.507	2.384	2.506	2.504	2.508	2.725	2.506	5.190	5.190	4.438
	RRMSE	20.2	19.8	20.2	19.2	20.2	20.2	20.3	22.0	20.2	41.9	41.9	35.8
	NS	0.896	0.901	0.896	0.906	0.897	0.897	0.896	0.878	0.897	0.556	0.556	0.675
	MAE	1.825	1.800	1.825	1.702	1.824	1.823	1.825	2.039	1.824	4.152	4.152	3.238
Shanghai	R^2	0.895**	0.916**	0.895**	0.923**	0.895**	0.895**	0.895**	0.861**	0.895**	0.536**	0.536**	0.573**
	RMSE	2.410	2.177	2.417	2.100	2.455	2.413	2.413	2.754	2.414	4.929	4.928	4.715
	RRMSE	18.8	17.0	18.8	16.4	19.1	18.8	18.8	21.5	18.8	38.4	38.4	36.8
	NS	0.888	0.908	0.887	0.915	0.884	0.888	0.888	0.854	0.888	0.531	0.531	0.571
	MAE	1.859	1.658	1.864	1.594	1.894	1.861	1.861	2.171	1.862	3.973	3.970	3.680
Average	R^2	0.900**	0.909**	0.900**	0.914**	0.900**	0.900**	0.900**	0.877**	0.900**	0.588**	0.588**	0.640**
	RMSE	2.494	2.397	2.494	2.325	2.510	2.480	2.497	2.720	2.458	4.982	4.982	4.582
	RRMSE	19.0	18.3	19.0	17.7	19.1	18.9	19.0	20.8	18.8	38.1	38.1	34.9
	NS	0.887	0.895	0.887	0.901	0.885	0.888	0.887	0.865	0.890	0.549	0.549	0.616
	MAE	1.885	1.812	1.885	1.730	1.898	1.872	1.887	2.086	1.851	4.010	4.009	3.499
	GPI	0.002	0.160	0.002	0.284	−0.021	0.022	−0.002	−0.388	0.053	−4.716	−4.715	−3.838
	Rank	5	2	6	1	8	4	7	9	3	12	11	10

Table 6: Statistics performances of the 12 models in estimating global solar radiation in South China.

Stations	Evaluation index	AP	OG	Jin	BA	LO	GM	EM	AH	DL	HS	AN	BC
	R^2	0.897**	0.902**	0.897**	0.911**	0.896**	0.897**	0.897**	0.871**	0.897**	0.613**	0.613**	0.705**
	RMSE	2.302	2.266	2.298	2.222	2.235	2.292	2.300	2.498	2.299	4.426	4.426	3.546
Guangzhou	RRMSE	17.8	17.6	17.8	17.2	17.3	17.8	17.8	19.4	17.8	34.3	34.3	27.5
	NS	0.868	0.872	0.868	0.877	0.875	0.869	0.868	0.844	0.868	0.510	0.510	0.686
	MAE	1.926	1.904	1.922	1.870	1.857	1.916	1.924	2.055	1.923	3.759	3.759	2.775
	R^2	0.882**	0.889**	0.882**	0.896**	0.882**	0.882**	0.882**	0.860**	0.882**	0.612**	0.612**	0.635**
	RMSE	2.725	2.669	2.729	2.554	2.727	2.727	2.721	2.951	2.724	5.190	5.190	4.753
Haikou	RRMSE	19.0	18.6	19.0	17.8	19.0	19.0	18.9	20.5	19.0	36.1	36.1	33.1
	NS	0.877	0.882	0.877	0.892	0.877	0.877	0.877	0.856	0.877	0.554	0.554	0.626
	MAE	2.173	2.105	2.175	2.007	2.175	2.174	2.170	2.399	2.172	4.249	4.249	3.764
	R^2	0.912**	0.921**	0.912**	0.927**	0.912**	0.912**	0.912**	0.886**	0.912**	0.732**	0.732**	0.748**
	RMSE	2.068	1.963	2.068	1.888	2.068	2.069	2.069	2.355	2.067	4.157	4.157	3.513
Nanning	RRMSE	16.7	15.8	16.7	15.2	16.7	16.7	16.7	19.0	16.7	33.5	33.5	28.3
	NS	0.911	0.920	0.911	0.926	0.911	0.911	0.911	0.885	0.911	0.642	0.642	0.744
	MAE	1.624	1.540	1.623	1.451	1.624	1.625	1.625	1.905	1.623	3.466	3.466	2.654
	R^2	0.897**	0.904**	0.897**	0.911**	0.897**	0.897**	0.897**	0.872**	0.897**	0.652**	0.652**	0.696**
	RMSE	2.365	2.299	2.365	2.222	2.343	2.363	2.363	2.601	2.363	4.591	4.591	3.937
	RRMSE	17.8	17.3	17.8	16.7	17.7	17.8	17.8	19.6	17.8	34.6	34.6	29.6
Average	NS	0.885	0.891	0.885	0.898	0.888	0.886	0.885	0.862	0.885	0.569	0.569	0.685
	MAE	1.908	1.850	1.907	1.776	1.885	1.905	1.906	2.119	1.906	3.825	3.825	3.064
	GPI	−0.001	0.127	−0.001	0.278	0.035	0.003	0.001	−0.473	0.001	−4.722	−4.722	−3.273
	Rank	8	2	7	1	3	4	6	9	5	12	11	10

Table 7: Statistics performances of the 12 models in estimating global solar radiation in Northeast China.

Stations	Evaluation index	AP	OG	Jin	BA	LO	GM	EM	AH	DL	HS	AN	BC
Harbin	R^2	0.900**	0.903**	0.900**	0.904**	0.900**	0.900**	0.900**	0.886**	0.900**	0.711**	0.711**	0.732**
	RMSE	2.816	2.770	2.826	2.789	2.818	2.819	2.822	3.006	2.835	4.061	4.061	3.941
	RRMSE	21.1	20.7	21.1	20.9	21.1	21.1	21.1	22.5	21.2	30.4	30.4	29.5
	NS	0.855	0.860	0.854	0.858	0.855	0.855	0.855	0.835	0.853	0.699	0.699	0.717
	MAE	2.132	2.089	2.141	2.106	2.134	2.134	2.137	2.298	2.149	3.062	3.062	2.939
Shenyang	R^2	0.909**	0.911**	0.909**	0.913**	0.909**	0.909**	0.909**	0.895**	0.909**	0.656**	0.656**	0.692**
	RMSE	2.226	2.209	2.223	2.181	2.225	2.223	2.222	2.360	2.228	4.310	4.310	4.096
	RRMSE	15.7	15.5	15.6	15.3	15.7	15.6	15.6	16.6	15.7	30.3	30.3	28.8
	NS	0.906	0.908	0.906	0.910	0.906	0.906	0.906	0.894	0.906	0.648	0.648	0.682
	MAE	1.628	1.629	1.626	1.595	1.628	1.626	1.624	1.712	1.630	3.357	3.357	3.140
Changchun	R^2	0.945**	0.945**	0.945**	0.946**	0.945**	0.945**	0.945**	0.934**	0.945**	0.680**	0.680**	0.731**
	RMSE	1.715	1.710	1.713	1.701	1.715	1.714	1.714	1.859	1.714	4.096	4.096	3.795
	RRMSE	12.7	12.7	12.7	12.6	12.7	12.7	12.7	13.8	12.7	30.4	30.4	28.2
	NS	0.944	0.944	0.944	0.945	0.944	0.944	0.944	0.934	0.944	0.679	0.679	0.724
	MAE	1.296	1.290	1.294	1.281	1.296	1.295	1.295	1.403	1.295	3.098	3.098	2.786
Average	R^2	0.918**	0.920**	0.918**	0.921**	0.918**	0.918**	0.918**	0.905**	0.918**	0.682**	0.682**	0.718**
	RMSE	2.252	2.230	2.254	2.224	2.253	2.252	2.253	2.408	2.259	4.156	4.156	3.944
	RRMSE	16.5	16.3	16.5	16.3	16.5	16.5	16.5	17.6	16.5	30.4	30.4	28.8
	NS	0.902	0.904	0.901	0.904	0.902	0.902	0.902	0.888	0.901	0.675	0.675	0.708
	MAE	1.685	1.669	1.687	1.661	1.686	1.685	1.686	1.805	1.691	3.172	3.172	2.955
	GPI	0.003	0.055	−0.001	0.072	0.002	0.003	0.002	−0.350	−0.011	−4.928	−4.928	−4.275
	Rank	3	2	7	1	5	4	6	9	8	12	11	10

TABLE 8: Statistics performances of the 12 models in estimating global solar radiation in Northwest China.

Stations	Evaluation index	AP	OG	Jin	BA	LO	GM	EM	AH	DL	HS	AN	BC
	R^2	0.859**	0.857**	0.859**	0.858**	0.859**	0.859**	0.859**	0.858**	0.859**	0.660**	0.660**	0.675**
	RMSE	3.319	3.332	3.317	3.327	3.321	3.321	3.318	3.349	3.318	4.999	4.999	4.887
Urumqi	RRMSE	23.1	23.2	23.1	23.2	23.1	23.2	23.1	23.3	23.1	34.8	34.8	34.1
	NS	0.849	0.848	0.849	0.848	0.849	0.849	0.849	0.846	0.849	0.657	0.657	0.672
	MAE	2.344	2.356	2.342	2.350	2.344	2.346	2.343	2.384	2.343	3.668	3.668	3.619
	R^2	0.872**	0.874**	0.872**	0.877**	0.872**	0.872**	0.872**	0.857**	0.872**	0.659**	0.659**	0.726**
	RMSE	2.955	2.915	2.966	2.897	2.973	2.961	2.953	3.106	2.955	4.721	4.721	4.104
Xian	RRMSE	24.2	23.9	24.3	23.7	24.3	24.2	24.2	25.4	24.2	38.6	38.6	33.6
	NS	0.853	0.857	0.852	0.859	0.852	0.853	0.854	0.838	0.853	0.626	0.626	0.717
	MAE	2.172	2.193	2.180	2.155	2.184	2.176	2.171	2.273	2.172	3.681	3.681	2.957
	R^2	0.934**	0.934**	0.934**	0.936**	0.934**	0.934**	0.934**	0.922**	0.934**	0.734**	0.734**	0.785**
	RMSE	1.808	1.806	1.807	1.771	1.807	1.809	1.807	1.969	1.807	3.594	3.594	3.233
Xining	RRMSE	11.6	11.5	11.6	11.3	11.6	11.6	11.6	12.6	11.6	23.0	23.0	20.7
	NS	0.932	0.932	0.932	0.935	0.932	0.932	0.932	0.920	0.932	0.732	0.732	0.783
	MAE	1.309	1.320	1.309	1.291	1.309	1.310	1.309	1.414	1.309	2.533	2.533	2.244
	R^2	0.888**	0.888**	0.888**	0.890**	0.888**	0.888**	0.888**	0.879**	0.888**	0.685**	0.685**	0.729**
	RMSE	2.694	2.684	2.697	2.665	2.700	2.697	2.693	2.808	2.693	4.438	4.438	4.075
	RRMSE	19.6	19.5	19.7	19.4	19.7	19.7	19.6	20.4	19.6	32.2	32.2	29.4
Average	NS	0.878	0.879	0.878	0.881	0.878	0.878	0.878	0.868	0.878	0.672	0.672	0.724
	MAE	1.942	1.956	1.944	1.932	1.946	1.944	1.941	2.024	1.941	3.294	3.294	2.940
	GPI	0.008	0.013	0.001	0.071	−0.006	0.001	0.010	−0.275	0.009	−4.929	−4.929	−3.787
	Rank	5	2	6	1	8	7	3	9	4	12	11	10

Table 9: Statistics performances of the 12 models in estimating global solar radiation in Southwest China.

Stations	Evaluation index	AP	OG	Jin	BA	LO	GM	EM	AH	DL	HS	AN	BC
Chengdu	R^2	0.875^{**}	0.891^{**}	0.875^{**}	0.901^{**}	0.875^{**}	0.875^{**}	0.875^{**}	0.844^{**}	0.875^{**}	0.760^{**}	0.760^{**}	0.820^{**}
	RMSE	2.771	2.600	2.794	2.550	2.774	2.779	2.772	3.039	2.786	3.697	3.697	2.830
	RRMSE	27.7	26.0	28.0	25.5	27.8	27.8	27.8	30.4	27.9	37.0	37.0	28.3
	NS	0.818	0.840	0.815	0.846	0.818	0.817	0.818	0.782	0.816	0.677	0.677	0.811
	MAE	2.249	2.089	2.269	2.049	2.252	2.256	2.249	2.481	2.262	2.913	2.913	2.152
Kunming	R^2	0.898^{**}	0.893^{**}	0.898^{**}	0.901^{**}	0.898^{**}	0.898^{**}	0.898^{**}	0.881^{**}	0.898^{**}	0.648^{**}	0.648^{**}	0.735^{**}
	RMSE	2.087	2.120	2.090	2.074	2.085	2.088	2.084	2.260	2.083	4.015	4.015	3.312
	RRMSE	12.8	13.0	12.9	12.8	12.8	12.8	12.8	13.9	12.8	24.7	24.7	20.4
	NS	0.894	0.890	0.893	0.895	0.894	0.894	0.894	0.875	0.894	0.606	0.606	0.732
	MAE	1.555	1.598	1.558	1.535	1.553	1.556	1.552	1.757	1.551	3.264	3.264	2.432
Lasa	R^2	0.911^{**}	0.911^{**}	0.911^{**}	0.911^{**}	0.911^{**}	0.911^{**}	0.911^{**}	0.907^{**}	0.911^{**}	0.670^{**}	0.670^{**}	0.702^{**}
	RMSE	1.759	1.769	1.773	1.772	1.761	1.771	1.764	1.785	1.767	2.972	2.972	2.863
	RRMSE	8.7	8.8	8.8	8.8	8.7	8.8	8.8	8.9	8.8	14.8	14.8	14.2
	NS	0.882	0.880	0.880	0.880	0.881	0.880	0.881	0.878	0.881	0.662	0.662	0.687
	MAE	1.247	1.251	1.258	1.259	1.248	1.256	1.250	1.311	1.253	2.235	2.235	2.072
Average	R^2	0.895^{**}	0.898^{**}	0.895^{**}	0.904^{**}	0.895^{**}	0.895^{**}	0.895^{**}	0.878^{**}	0.895^{**}	0.693^{**}	0.693^{**}	0.753^{**}
	RMSE	2.206	2.163	2.219	2.132	2.207	2.212	2.206	2.361	2.212	3.561	3.561	3.002
	RRMSE	16.4	16.0	16.5	15.7	16.4	16.5	16.4	17.7	16.5	25.5	25.5	21.0
	NS	0.865	0.870	0.863	0.874	0.864	0.864	0.864	0.845	0.864	0.648	0.648	0.743
	MAE	1.684	1.646	1.695	1.614	1.684	1.689	1.684	1.850	1.689	2.804	2.804	2.218
	GPI	0.019	0.172	−0.019	0.290	0.016	0.000	0.017	−0.529	0.000	−4.710	−4.710	−2.662
	Rank	3	2	8	1	5	6	4	9	7	11	12	10

16.4%, average MAE of 1.614, 1.646, and 1.684 MJ m^{-2} d^{-1}, average NS of 0.874, 0.870, and 0.865, and GPI of 0.290, 0.172, and 0.019, respectively. The BC model showed the best performance among the temperature-based models, with average R^2 of 0.753, average RMSE of 3.002 MJ m^{-2} d^{-1}, average RRMSE of 21.0%, average MAE of 2.218 MJ m^{-2} d^{-1}, average NS of 0.743, and GPI of −2.662.

Comparison between estimated and measured monthly average daily R_s and relative error (RE) of different models for each subzone are presented in Figure 2. As shown in Figure 2, the estimated and measured monthly average daily R_s had good agreements. In addition to Wuhan, Nanchang, Shanghai, Chengdu, and Kunming stations, the estimated and measured R_s all presented parabolic variation. For the 9 sunshine-based models (AP, OG, Jin, BA, LO, GM, EM, AH, and DL), the average RE was in the range 1.71%~12.94%, 1.59%~12.72%, 1.71%~13.38%, 1.61%~13.17%, 1.67%~12.98%, 1.74%~13.09%, 1.70%~12.95%, 1.93%~13.19%, and 1.68%~13.20%, respectively. For the 3 temperature-based models (HS, AN, and BC), the average RE was in the range 3.33%~21.96%, 3.33%~21.96%, and 3.18%~15.16%, respectively. This means the sunshine-based models had a better performance for monthly average daily R_s compared with the temperature-based models, and the OG model had the lowest RE value between the sunshine-based models, followed by DL and GM models, with average RE of 5.66%, 5.73%, and 5.80%. In the temperature-based models, BC model had the lowest RE value, with average RE of 8.26%, and the RE of HS and AN models RE had a large variation in a year. For the 7 subzones (North China, Central China, East China, South China, Northeast China, Northwest China, and Southwest China), the models with the lowest RE were Jin, OG, DL, LO, AP, OG, and HS models, respectively, with average RE of 4.87%, 6.77%, 4.79%, 4.81%, 5.71%, 5.09%, and 5.08%. In Taiyuan, Jinan, Harbin, and Chengdu stations, all the models trended to underestimate the monthly average daily R_s. Overall, there were large differences for models in under/overestimating R_s at different climatic zones.

4. Discussion

Results indicated that the prediction accuracy of each model for estimating R_s was different in each subzone of China. This may be due to the vast territory of China, which leads to a wide difference of topography and climate in different areas. Generally, the sunshine-based models had a better performance for the 7 subzones compared with the temperature-based models. Trnka et al. [41] analyzed 7 methods for estimating daily R_s in the Central Europe case study area (lowlands of Austria and the Czech Republic), where the sunshine-based models were found to be the best of all tested models, followed by cloud-based models, precipitation-based models, and temperature-based models. Mecibah et al. [42] introduced the best model for predicting the monthly mean daily R_s on a horizontal surface for 6 Algerian cities, and the results obtained in this study confirmed the previous studies, which indicated that the sunshine-based models were generally more accurate to estimate R_s than temperature-based models. The amount of solar radiation reaching the earth's surface is closely related to sunshine duration. At the same time, clouds and their accompanying weather patterns are also one of the most important atmospheric phenomena that restrict the solar radiation on the earth's surface, and this is the main reason for the higher accuracy of the sunshine-based models and cloud-based models. Solar radiation reaching the earth's surface is absorbed by the atmosphere or emitted into the air in the form of long wave radiation, and the portion absorbed by the atmosphere causes an increase in atmospheric temperature. Therefore, the effect of temperature on solar radiation is less than sunshine duration, which led to the lower calculation accuracy of the temperature-based models compared with sunshine-based models.

In addition, the present study found that Bahel model showed the best estimation precision of R_s in the 7 subzones. Chelbi et al. [16] compared several Ångström-type regression models, namely, the linear, quadratic, cubic, logarithmic, and exponential models, in Tunisia, and the results showed that the cubic model (Bahel model) showed the best regression fit and performed slightly better. Chen et al. [43] compared 5 R_s models with measured daily data in China; the results showed that the estimated daily R_s was relatively accurate using sunshine-based models, and the Bahel model was slightly better than the Ångström model with average NS of 0.84 and 0.83, respectively. This research found that the BC model had the best estimation precision for R_s between the temperature-based models. Quej et al. [17] evaluated the prediction accuracy and applicability of 13 empirical R_s models for warm subhumid regions (Yucatán Peninsula, Mexico), and results showed that the BC model was the best temperature-based model for estimating R_s. Chen et al. [43] also found that the BC model was more accurate for R_s than HS model, with average NS of 0.47 and 0.44, respectively. This is consistent with the results in the present study. In addition, we should analyze the influence of different geographical and meteorological factors on the accuracy of different models.

5. Conclusion

In this study, 12 solar radiation models were evaluated using daily meteorological data for estimating R_s at 21 meteorological stations across China. The performance of each model has been evaluated and compared using the RMSE, RRMSE, NS, MAE, RE, and GPI. The main conclusions of this study are shown as follows.

(1) The estimated and measured daily R_s had statistically significant correlations ($P < 0.01$) for all models at 21 meteorological stations. The sunshine-based models were more accurate for R_s estimation than the temperature-based models. For the 7 subzones, the BA model had the best estimation precision for daily R_s estimation among the 12 models. In China, the BA model also showed the best daily R_s estimation compared with other sunshine-based models, followed by OG and DL models, with average R^2 of 0.910, 0.905, and 0.902, average RMSE of 2.306, 2.352, and 2.386 MJ m^{-2} d^{-1}, average RRMSE of 17.3%, 17.7%, and 17.9%, average MAE of 1.724, 1.775, and 1.799 MJ m^{-2} d^{-1}, average NS of 0.895, 0.891,

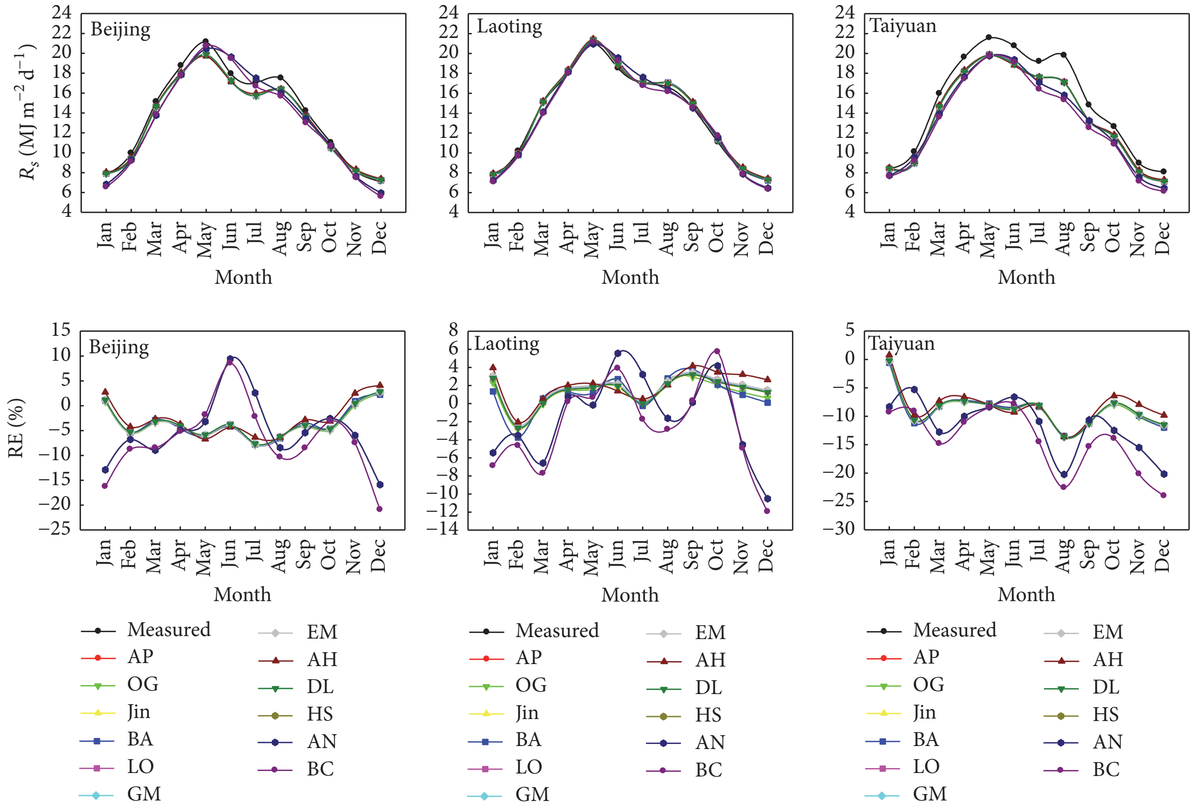

(a) North China

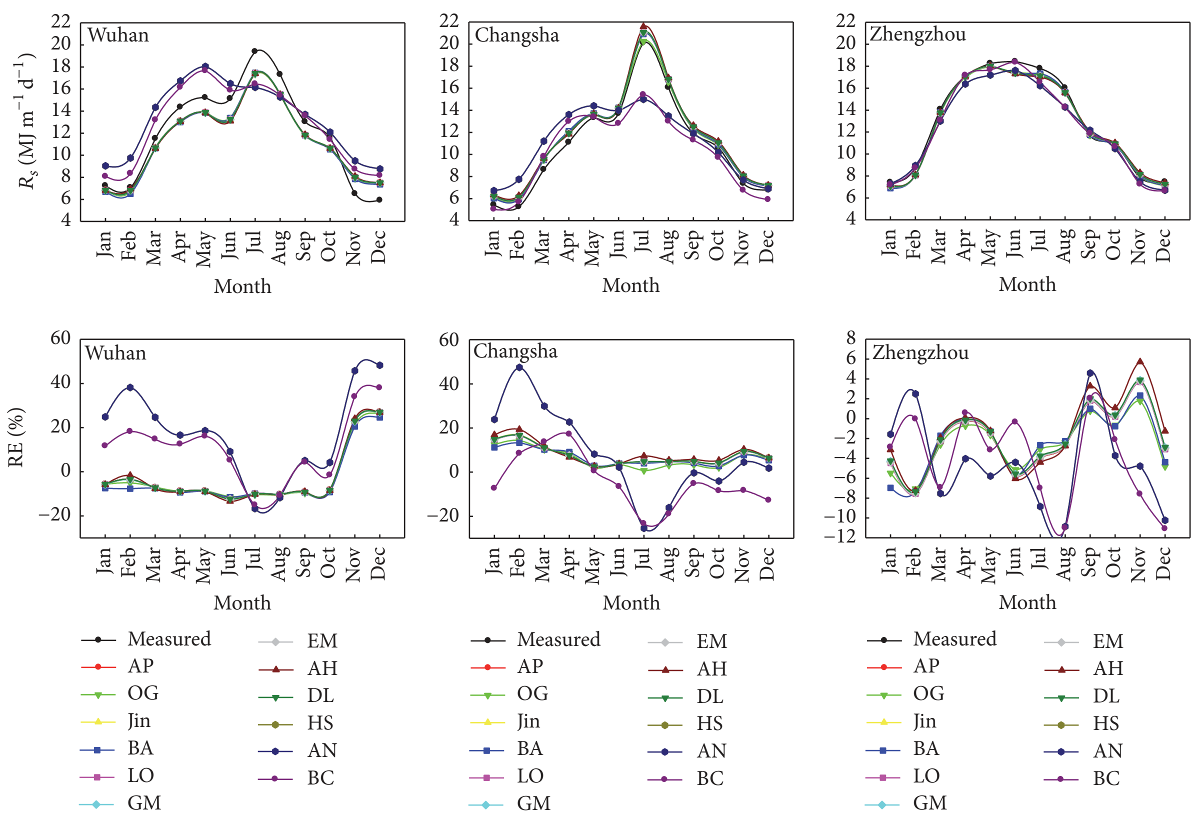

(b) Central China

Figure 2: Continued.

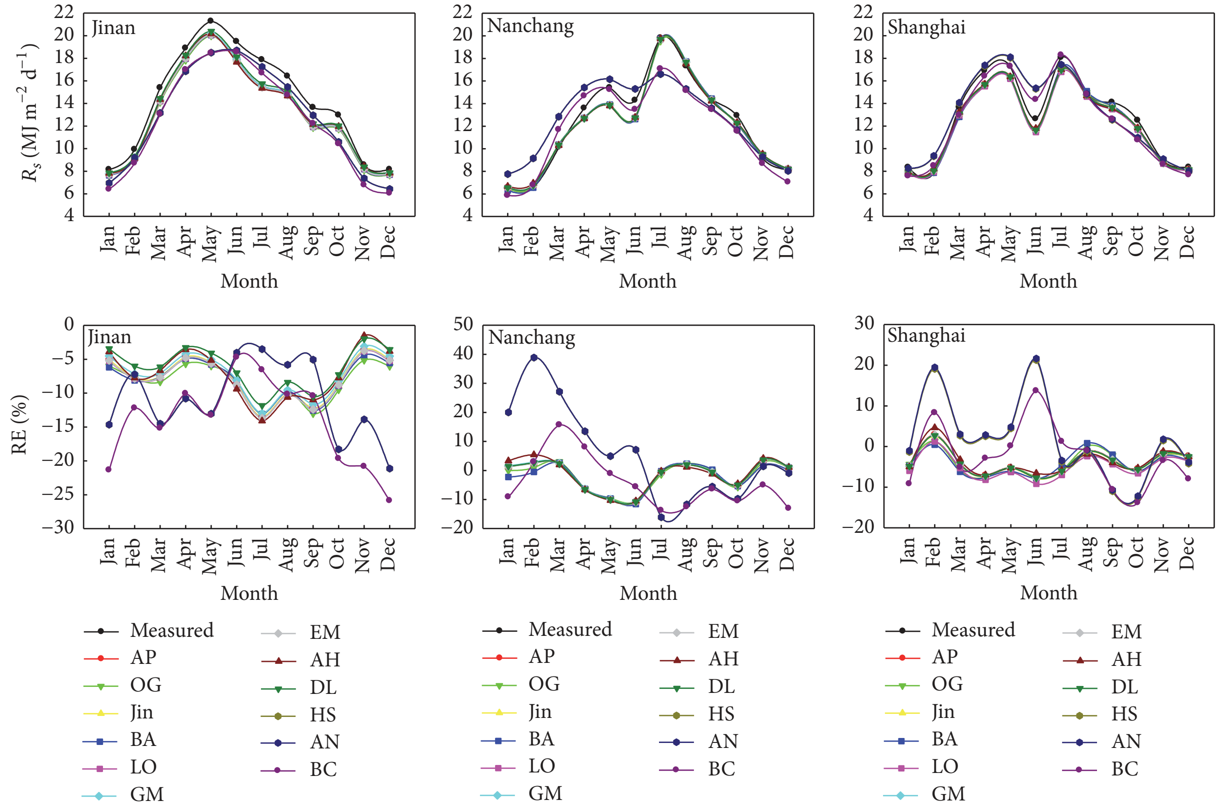

(c) East China

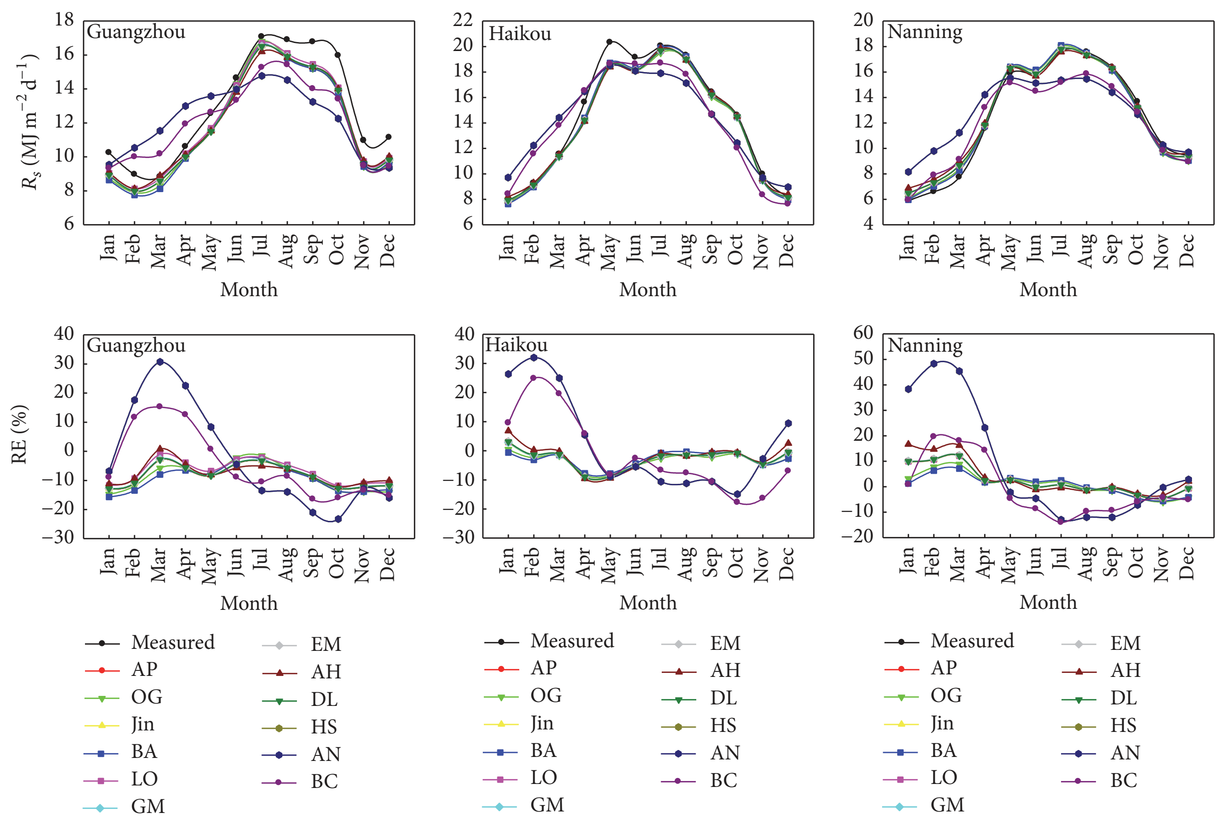

(d) South China

FIGURE 2: Continued.

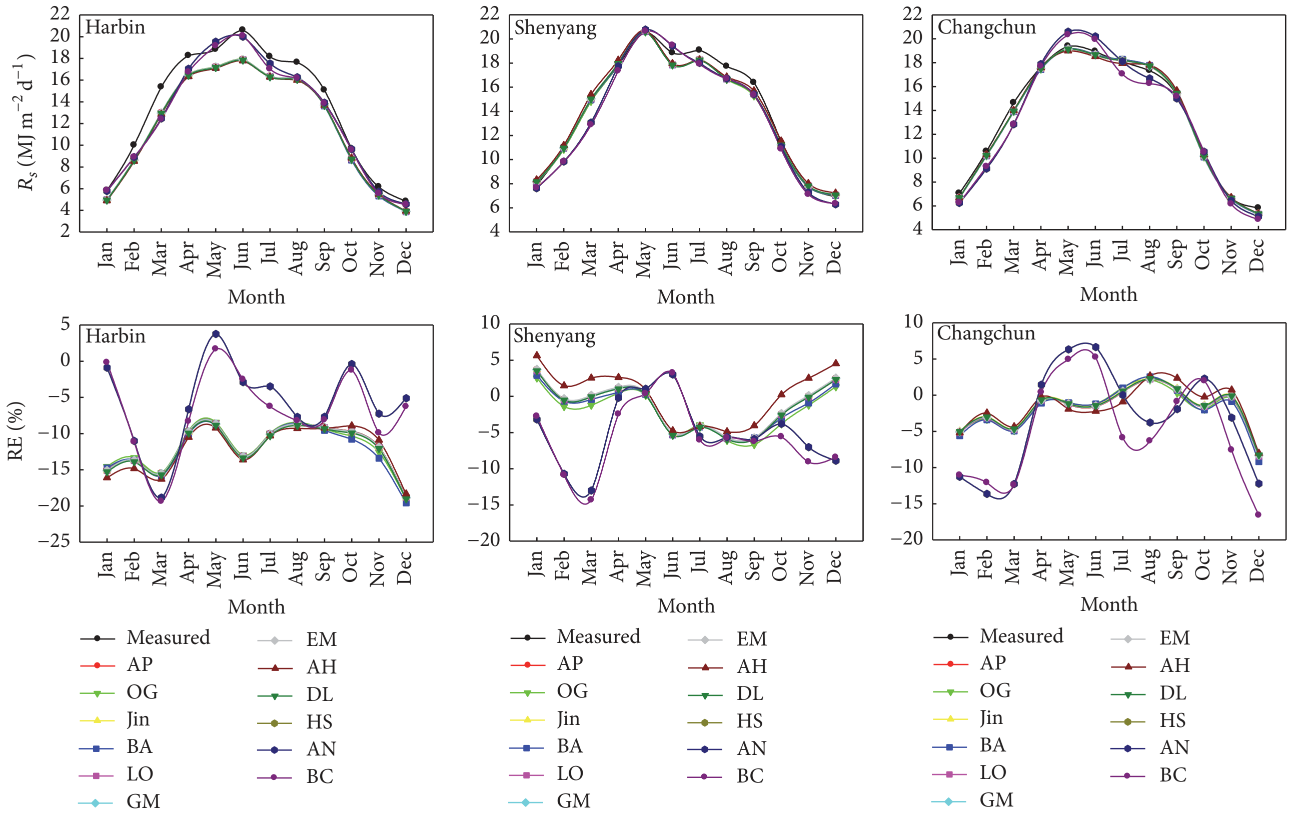

(e) Northeast China

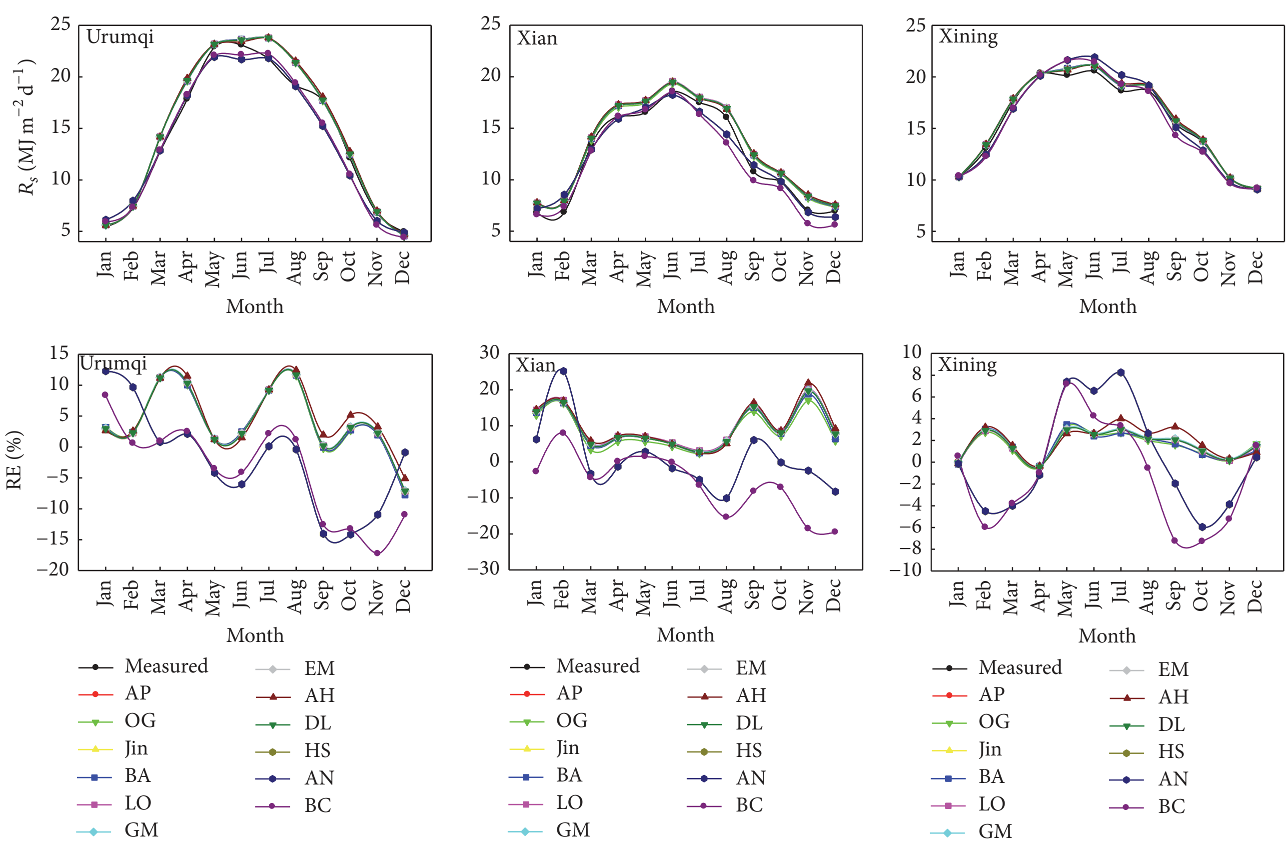

(f) Northwest China

Figure 2: Continued.

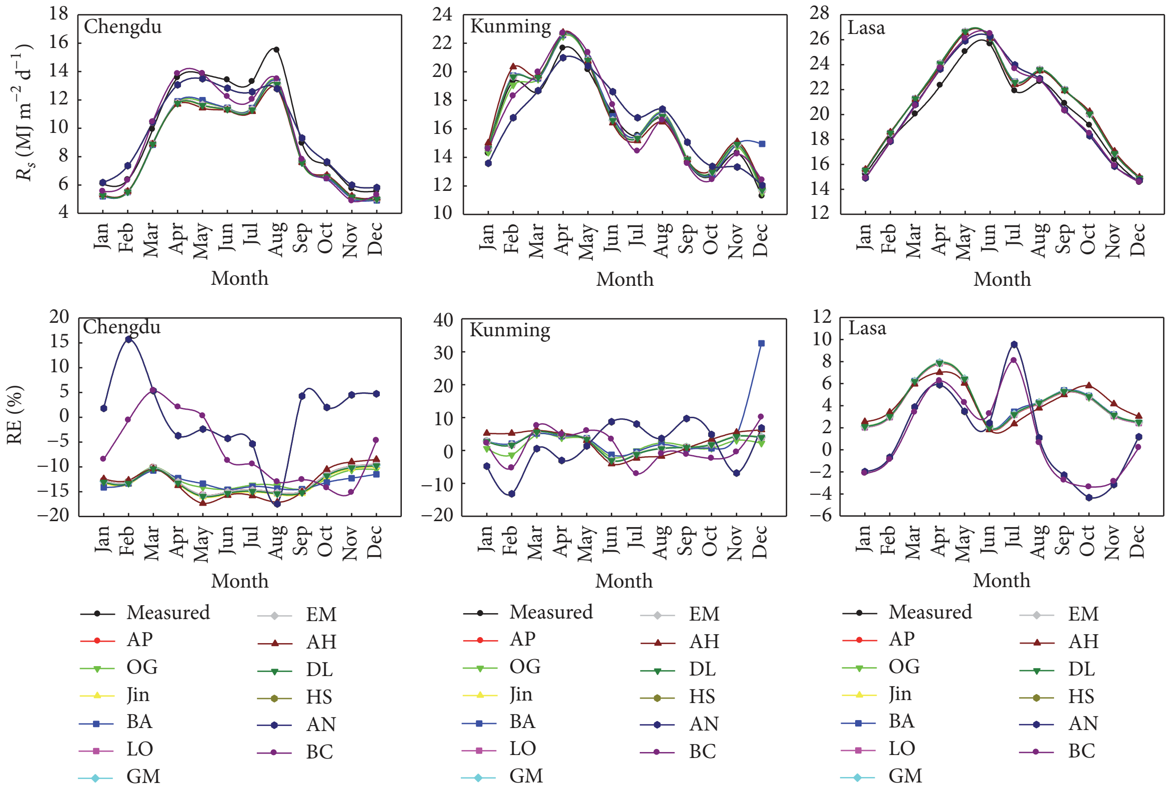

(g) Southwest China

Figure 2: Comparison between monthly average daily global solar radiation and relative error of each model in China.

and 0.887, and GPI of 0.191, 0.084, and 0.008, respectively. The BC model had the best estimation accuracy among the temperature-based models, with average R^2 of 0.710, average RMSE of 3.952 MJ m^{-2} d^{-1}, average RRMSE of 29.5%, average MAE of 2.958 MJ m^{-2} d^{-1}, average NS of 0.696, and GPI of −3.650, respectively.

(2) At monthly scale, the sunshine-based models also had a better performance compared with the temperature-based models for monthly average daily R_s estimation, and the OG model had the lowest RE value between the sunshine-based models, followed by DL and GM models, with average RE of 5.66%, 5.73%, and 5.80%. In the temperature-based models, the BC model had the lowest RE value, with average RE of 8.26%. For the 7 subzones (North China, Central China, East China, South China, Northeast China, Northwest China, and Southwest China), the models with the lowest RE are Jin, OG, DL, LO, AP, OG, and HS models, respectively, with average RE of 4.87%, 6.77%, 4.79%, 4.81%, 5.71%, 5.09%, and 5.08%.

(3) Overall, the BA model is recommended to estimate daily R_s and the OG model is recommended to estimate monthly average daily R_s in China when the sunshine hours are available, and the BC model is recommended to estimate both daily R_s and monthly average daily R_s when only temperature data are available.

Complete and accurate R_s data at a specific region are highly crucial to regional crop growth modeling, irrigation system development and utilization of solar energy resources. The main objective of this study is to evaluate the applicability of different radiation models in 7 subzones of China. When sunlight passes through the atmosphere, a portion of sunlight is scattered, reflected, or absorbed by gases, clouds, and dust in the atmosphere, which varies with time in temperature and composition. Unfortunately, our work ignored the question and did not take into account the effects of climate change and human activities on solar radiation. We mainly consider the application of clean energy in agricultural production, and we will take into account this question in the future research.

Conflicts of Interest

The authors declare that they have no conflicts of interest.

Acknowledgments

The authors would like to thank the National Climatic Centre of the China Meteorological Administration for providing the climate database used in this study. This work was also supported by the National Key Research and Development Program of China (no. 2016YFC0400206), National Natural Science Foundation of China (51779161), and National Key Technologies R&D Program of China (no. 2015BAD24B01).

References

[1] J. Almorox, M. Bocco, and E. Willington, "Estimation of daily global solar radiation from measured temperatures at Cañada de Luque, Córdoba, Argentina," *Journal of Renewable Energy*, vol. 60, pp. 382–387, 2013.

[2] S. Mehdizadeh, J. Behmanesh, and K. Khalili, "Comparison of artificial intelligence methods and empirical equations to estimate daily solar radiation," *Journal of Atmospheric and Solar-Terrestrial Physics*, vol. 146, pp. 215–227, 2016.

[3] G. E. Hassan, M. E. Youssef, M. A. Ali, Z. E. Mohamed, and A. I. Shehata, "Performance assessment of different day-of-the-year-based models for estimating global solar radiation—case study: Egypt," *Journal of Atmospheric and Solar-Terrestrial Physics*, vol. 149, pp. 69–80, 2016.

[4] B. Jamil and N. Akhtar, "Estimation of diffuse solar radiation in humid-subtropical climatic region of India: Comparison of diffuse fraction and diffusion coefficient models," *Energy*, vol. 131, pp. 149–164, 2017.

[5] A. K. Katiyar and C. K. Pandey, "Simple correlation for estimating the global solar radiation on horizontal surfaces in India," *Energy*, vol. 35, no. 12, pp. 5043–5048, 2010.

[6] F. Besharat, A. A. Dehghan, and A. R. Faghih, "Empirical models for estimating global solar radiation: a review and case study," *Renewable & Sustainable Energy Reviews*, vol. 21, pp. 798–821, 2013.

[7] T. Pan, S. Wu, E. Dai, and Y. Liu, "Estimating the daily global solar radiation spatial distribution from diurnal temperature ranges over the tibetan plateau in China," *Applied Energy*, vol. 107, pp. 384–393, 2013.

[8] L. A. Hunt, L. Kuchar, and C. J. Swanton, "Estimation of solar radiation for use in crop modelling," *Agricultural and Forest Meteorology*, vol. 91, no. 3-4, pp. 293–300, 1998.

[9] M. G. Abraha and M. J. Savage, "Comparison of estimates of daily solar radiation from air temperature range for application in crop simulations," *Agricultural and Forest Meteorology*, vol. 148, no. 3, pp. 401–416, 2008.

[10] X. Liu, X. Mei, Y. Li et al., "Evaluation of temperature-based global solar radiation models in China," *Agricultural and Forest Meteorology*, vol. 149, no. 9, pp. 1433–1446, 2009.

[11] G. E. Hassan, M. E. Youssef, Z. E. Mohamed, M. A. Ali, and A. A. Hanafy, "New temperature-based models for predicting global solar radiation," *Applied Energy*, vol. 179, pp. 437–450, 2016.

[12] J. Piri and O. Kisi, "Modelling solar radiation reached to the Earth using ANFIS, NN-ARX, and empirical models (Case studies: Zahedan and Bojnurd stations)," *Journal of Atmospheric and Solar-Terrestrial Physics*, vol. 123, pp. 39–47, 2015.

[13] S. S. Sharifi, V. Rezaverdinejad, and V. Nourani, "Estimation of daily global solar radiation using wavelet regression, ANN, GEP and empirical models: a comparative study of selected temperature-based approaches," *Journal of Atmospheric and Solar-Terrestrial Physics*, vol. 149, pp. 131–145, 2016.

[14] A. Ångström, "Solar and terrestrial radiation. Report to the international commission for solar research on actinometric investigations of solar and atmospheric radiation," *Quarterly Journal of the Royal Meteorological Society*, vol. 50, no. 210, pp. 121–126, 1924.

[15] J. A. Prescott, "Evaporation from water surface in relation to solar radiation," *Transactions of the Royal Society of South Australia*, vol. 64, pp. 114–118, 1940.

[16] M. Chelbi, Y. Gagnon, and J. Waewsak, "Solar radiation mapping using sunshine duration-based models and interpolation techniques: application to Tunisia," *Energy Conversion and Management*, vol. 101, pp. 203–215, 2015.

[17] V. H. Quej, J. Almorox, M. Ibrakhimov, and L. Saito, "Empirical models for estimating daily global solar radiation in Yucatán Peninsula, Mexico," *Energy Conversion and Management*, vol. 110, pp. 448–456, 2016.

[18] J. Almorox, V. H. Quej, and P. Martí, "Global performance ranking of temperature-based approaches for evapotranspiration estimation considering Köppen climate classes," *Journal of Hydrology*, vol. 528, pp. 514–522, 2015.

[19] G. H. Hargreaves and Z. A. Samani, "Estimating potential evapotranspiration," *Journal of the Irrigation & Drainage Division*, vol. 108, no. 3, pp. 225–230, 1982.

[20] J. Annandale, N. Jovanovic, N. Benadé, and R. Allen, "Software for missing data error analysis of Penman-Monteith reference evapotranspiration," *Irrigation Science*, vol. 21, no. 2, pp. 57–67, 2002.

[21] R. G. Allen, "Self-calibrating method for estimating solar radiation from air temperature," *Journal of Hydrologic Engineering*, vol. 2, no. 2, pp. 56–67, 1997.

[22] R. Allen, *Evaluation of Procedures of Estimating Mean Monthly Solar Radiation from Air Temperature*, FAO, Rome, Italy, 1995.

[23] K. L. Bristow and G. S. Campbell, "On the relationship between incoming solar radiation and daily maximum and minimum temperature," *Agricultural and Forest Meteorology*, vol. 31, no. 2, pp. 159–166, 1984.

[24] D. G. Goodin, J. M. S. Hutchinson, R. L. Vanderlip, and M. C. Knapp, "Estimating solar irradiance for crop modeling using daily air temperature data," *Agronomy Journal*, vol. 91, no. 5, pp. 845–851, 1999.

[25] Z. A. Al-Mostafa, A. H. Maghrabi, and S. M. Al-Shehri, "Sunshine-based global radiation models: a review and case study," *Energy Conversion and Management*, vol. 84, pp. 209–216, 2014.

[26] J. Almorox, C. Hontoria, and M. Benito, "Models for obtaining daily global solar radiation with measured air temperature data in Madrid (Spain)," *Applied Energy*, vol. 88, no. 5, pp. 1703–1709, 2011.

[27] X. Liu, X. Mei, Y. Li, Q. Wang, Y. Zhang, and J. R. Porter, "Variation in reference crop evapotranspiration caused by the Ångström-Prescott coefficient: locally calibrated versus the FAO recommended," *Agricultural Water Management*, vol. 96, no. 7, pp. 1137–1145, 2009.

[28] H. Ögelman, A. Ecevit, and E. Tasdemiroğlu, "A new method for estimating solar radiation from bright sunshine data," *Solar Energy*, vol. 33, no. 6, pp. 619–625, 1984.

[29] Z. Jin, W. Yezheng, and Y. Gang, "General formula for estimation of monthly average daily global solar radiation in China," *Energy Conversion and Management*, vol. 46, no. 2, pp. 257–268, 2005.

[30] V. Bahel, H. Bakhsh, and R. Srinivasan, "A correlation for estimation of global solar radiation," *Energy*, vol. 12, no. 2, pp. 131–135, 1987.

[31] A. Louche, G. Notton, P. Poggi, and G. Simonnot, "Correlations for direct normal and global horizontal irradiation on a French Mediterranean site," *Solar Energy*, vol. 46, no. 4, pp. 261–266, 1991.

[32] J. Glover and J. S. G. McCulloch, "The empirical relation between solar radiation and hours of sunshine," *Quarterly Journal of the Royal Meteorological Society*, vol. 84, no. 360, pp. 172–175, 1958.

[33] N. A. Elagib and M. G. Mansell, "New approaches for estimating global solar radiation across Sudan," *Energy Conversion and Management*, vol. 41, no. 5, pp. 419–434, 2000.

[34] J. Almorox and C. Hontoria, "Global solar radiation estimation using sunshine duration in Spain," *Energy Conversion and Management*, vol. 45, no. 9-10, pp. 1529–1535, 2004.

[35] R. Dogniaux and M. Lemoine, "Classification of radiation sites in terms of different indices of atmospheric transparency," *Solar Energy Research and Development in the European Community*, vol. 2, pp. 94–107, 1983.

[36] G. H. Hargreaves, "Simplified coefficients for estimating monthly solar radiation," in *North America and Europe, Departmental paper, Departmental of Biological and Irrigation Engineering*, Utah State University, 1994.

[37] Y. Feng, N. Cui, D. Gong, Q. Zhang, and L. Zhao, "Evaluation of random forests and generalized regression neural networks for daily reference evapotranspiration modelling," *Agricultural Water Management*, vol. 193, pp. 163–173, 2017.

[38] Y. Feng, Y. Jia, N. Cui, L. Zhao, C. Li, and D. Gong, "Calibration of Hargreaves model for reference evapotranspiration estimation in Sichuan basin of southwest China," *Agricultural Water Management*, vol. 181, pp. 1–9, 2017.

[39] M. Despotovic, V. Nedic, D. Despotovic, and S. Cvetanovic, "Review and statistical analysis of different global solar radiation sunshine models," *Renewable & Sustainable Energy Reviews*, vol. 52, pp. 1869–1880, 2015.

[40] J. B. Boisvert, H. N. Hayhoe, and P. A. Dubé, "Improving the estimation of global solar radiation across Canada," *Agricultural and Forest Meteorology*, vol. 52, no. 3-4, pp. 275–286, 1990.

[41] M. Trnka, Z. Žalud, J. Eitzinger, and M. Dubrovský, "Global solar radiation in Central European lowlands estimated by various empirical formulae," *Agricultural and Forest Meteorology*, vol. 131, no. 1-2, pp. 54–76, 2005.

[42] M. S. Mecibah, T. E. Boukelia, R. Tahtah, and K. Gairaa, "Introducing the best model for estimation the monthly mean daily global solar radiation on a horizontal surface (Case study: Algeria)," *Renewable & Sustainable Energy Reviews*, vol. 36, pp. 194–202, 2014.

[43] R. Chen, K. Ersi, J. Yang, S. Lu, and W. Zhao, "Validation of five global radiation models with measured daily data in China," *Energy Conversion and Management*, vol. 45, no. 11-12, pp. 1759–1769, 2004.